Journal of The Electrochemical Society, **155** (2) B163-B171 (2008)
0013-4651/2007/155(2)/B163/9/$23.00 © The Electrochemical Society

State of Water in Perfluorosulfonic Ionomer (Nafion 117) Proton Exchange Membranes

Zijie Lu,[a,b,*] Georgios Polizos,[a] Digby D. Macdonald,[b,,z] and E. Manias[a,z]**

[a]*Polymer Nanostructures Laboratory, Center for the Study of Polymeric Systems, and* [b]*Center for Electrochemical Science and Technology, Department of Materials Science and Engineering, Pennsylvania State University, University Park, Pennsylvania 16802, USA*

The nature of water in acid-form Nafion 117 was quantified at several hydration levels by dielectric relaxation spectroscopy. Two independent experimental setups were used to collect complex dielectric permittivity spectra at low frequencies (0.01 Hz to 1 MHz at −80 to 25°C) and in the microwave region (0.40–26 GHz at 25–45°C). We directly observed the states of water, manifested through three population averages with distinctly resolved dynamical behaviors, and their changes with temperature and hydration level. The fastest process observed was identified as the cooperative picosecond relaxation of free (isotropic, bulklike) water, whereas the slowest process (microsecond relaxation times) corresponded to water molecules strongly bound to the charged sulfonic groups. A third type of water was also observed, also characterized by picosecond relaxation times, close to and about three times slower than those of bulk water, which was attributed to loosely bound water and may contain substantial dynamical heterogeneities.
 [DOI: 10.1149/1.2815444]

Manuscript received August 21, 2007. Available electronically December 12, 2007.

Extensive studies have been performed on perfluorinated ionomers[1-4] because of their increasing application in fuel cell devices. Nafion, developed and commercialized by DuPont, is a perfluorosulfonated ionomer used as both a separator and an electrolyte in proton exchange membrane (PEM) fuel cells in automotive and stationary applications.[5] Its chemical structure, consisting of a tetrafluoroethylene backbone bearing sulfonate-terminated perfluorovinyl ether branches, offers thermomechanical stability and at the same time allows for the formation of hydrophilic domains that can accommodate hydrated protons. Water facilitates the motion of protons through the polymer matrix[6-9] and thus the water content and water dynamics determine PEM properties such as proton conductivity,[6,7,10-14] methanol and oxygen permeability,[6,15-17] and electro-osmotic drag.[6,18-20]

The phase-separated morphology of the polymer matrix, consisting of nanometer-sized hydrophilic and hydrophobic (ion-rich and fluorocarbon) domains,[21] gives rise to a variety of environments where water exists; these local environments relate not only to the structure of the polymeric membrane but also to the strong polymer/water interactions,[22-27] cf. ion–dipole and dipole–dipole. Thus, it is expected that a commensurate variety of water "states" will also develop, i.e., local water environments with structures, and especially with dynamics, being determined by a combination of geometric factors and intermolecular interactions. Along these lines, different water states have been proposed to exist in Nafion membranes (for a detailed review see, for example, Paddison et al.[10-12] and references therein) corresponding to different environments. Namely, water molecules that do not interact strongly with the polymer matrix would exhibit liquid-water dynamics, whereas water bound to the polymer hydrophilic groups, those located at the polymer/liquid-water interface or trapped within the fluorocarbon chains, would exhibit slower dynamics. In order of decreasing hydrogen-bonding strength to the polymer, three types of water were suggested: bulklike (not hydrogen bonded to the polymer), weakly hydrogen bonded ("loosely bound" to the polymer), and strongly hydrogen bonded water to the sulfonate groups ("bound" water).[8,28,29] In concert, differential scanning calorimetry measurements suggest different responses for these three waters, with bulklike water freezing at about 0°C, the loosely bound water displaying a broad endothermic peak at lower temperatures, and the strongly bound water showing an inability to freeze,[25,30-34] termed as "free", "freezable loosely bound", and "nonfreezing" water, respectively,[4,8,25] similar to polymer hydrogels. Nuclear magnetic resonance studies[35-38] indicated a distribution of water environments, with a measurably fast exchange of water molecules between different environments and sites and with the population of the fast relaxing states increasing with water content in the polymer.

Broadband dielectric relaxation spectroscopy (DRS) studies reported a bimodal relaxation suggesting the existence of water in diverse hydrated clusters.[39,40] Similar approaches in K^+ exchanged Nafion membranes[41,42] reported a broad dielectric relaxation around 50 kHz at 25°C, which was also attributed to the same sulfonate-water complexes. However, these investigations were limited to low frequencies ($f < 10$ MHz) and, consequently, do not provide any description of the freezable states of water within the membranes. Microwave DRS can explore the relevant time scales of these latter water states, and recent work, e.g., 0.045–30 GHz spectra of Nafion 117,[43,44] showed a strong dependence of the dielectric constant and of the loss factors on the water content, although those reflection spectra could not obtain any detailed information about discrete water relaxations (states of water).

In view of the above, it becomes clear that the dynamic states of water in Nafion membranes remain still largely unclear. Here, we report a DRS study of hydrated Nafion 117 in the acid form over a wide frequency range, aiming to elucidate the dynamics and the nature of water in these membranes.

Experimental

Sample preparation.— Nafion 117 membranes (DuPont, equivalent weight = 1100 g/equiv) were treated as in previous studies:[19,43,45] boiling in 3% H_2O_2, rinsing in boiling water, then boiling in 0.5 M H_2SO_4, and finally rinsing in boiling water (at least 1 h for each step). In order to prepare membrane samples of known water content, the pretreated Nafion 117 membranes were suspended

Table I. Conditions of membrane equilibration (at 25°C): water content set values (λ, water molecules per sulfonic acid) and the corresponding aqueous solutions and relative humidities used.

Solution	Relative humidity (%)	Water content (λ)
Saturated water vapor	100	12
1 mol/kg LiCl solution	96	9
Saturated NaCl solution	75	6
Saturated $MgCl_2$ solution	33	3
Dried (120°C, vacuum, 12 h)	0	0

* Electrochemical Society Student Member.
** Electrochemical Society Fellow.
z E-mail: ddm2@psu.edu; manias@psu.edu

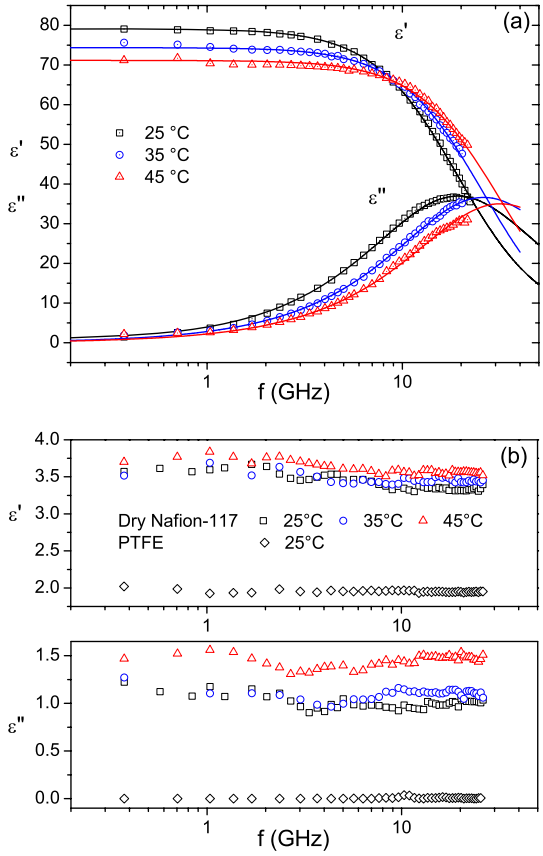

Figure 1. (Color online) Microwave dielectric relaxation transmission-mode spectra of (a) liquid water and (b) dry Nafion 117 and polytetrafluoroethylene. The solid lines through the water dielectric spectra are Debye relaxation fits.

in a closed container, where the relative humidity was controlled by various solutions. Table I shows the selected solutions, the relative humidity, and the water content achieved (λ denotes the number of absorbed water molecules per -SO_3H site of the membrane). Care was taken to ensure equilibration of the Nafion membrane at the desired hydration levels, λ. This was accomplished by starting from a low water content membrane, e.g., λ = 1 or 2, and suspending it for several days in a chamber with appropriate relative humidity (Table I), selected based on previous detailed studies of water uptake for the same membrane;[46] subsequently, the specimen was weighed to measure/confirm its water content, oftentimes requiring further equilibration in the same chamber if the desired λ was not achieved.

Broadband DRS.— Complex dielectric permittivity, $\varepsilon^*(\omega)$ [defined as $\varepsilon^*(\omega) = \varepsilon'(\omega) - i\varepsilon''(\omega)$, where ε' is the real (dielectric dispersion) and ε'' is the imaginary (dielectric loss) part of the permittivity] was measured by employing broadband DRS in the frequency range 10^{-2}–10^7 Hz. A disklike specimen, 20 mm diam and 0.17 mm thick, was sandwiched between gold-coated brass electrodes and mounted on a ZGS Alpha active sample cell connected to a Novocontrol Alpha analyzer. Measurements were performed isothermally from 25 to −80°C. Temperature was controlled by a Quatro Cryosystem (operated with liquid nitrogen) with a nominal temperature stabilization of ±0.2°C.

Microwave DRS.— The dielectric relaxations of hydrated Nafion 117 membranes were also measured at microwave frequencies by collecting transmission spectra with an HP8510C network analyzer (frequency range: 45 MHz to 26 GHz). Nafion membranes, pretreated as described above, were wrapped around the inner conductor of a 10 cm coaxial airline used as a waveguide. Transmission-mode spectra were collected, rather than reflection spectra, due to the better sensitivity in probing relaxations in these systems. Interactions between the travelling waves and the membrane material affect the magnitude of the transmitted wave, with the ratio of transmitted to incident wave voltage defined as the scattering parameter, S_{21}, which is related to the complex permittivity $[\varepsilon^*(\omega) = \varepsilon'(\omega) - i\varepsilon''(\omega)]$ of the material.[47-49] No analytical expression for $\varepsilon^*(\omega)$ can be obtained, and $\varepsilon'(\omega)$ and $\varepsilon''(\omega)$ were calculated numerically[48,49] from the measured S_{21}. The experimental setup, the measurement and analysis procedures, and the related uncertainties are described in detail elsewhere.[46,48,49] The microwave DRS measurements were carried out at five temperatures, 25, 30, 35, 40, and 45°C, and the temperature was controlled to a precision of ±0.2°C.

Microwave DRS of liquid (bulk) water and of dry Nafion 117.— In order to assess the validity of our microwave DRS for determining the dielectric response of hydrated Nafion, we first performed microwave DRS measurements on liquid water. The dielectric spectra (ε' and ε'' vs frequency, $f = \omega/2\pi$) of bulk/liquid water are presented in Fig. 1a, and the best fittings to the raw data are obtained by a single Debye function. Relaxation times of 8.30, 6.48, and 5.17 ps were obtained for liquid water at T = 25, 35, and 45°C, respectively. These relaxation times are in excellent agreement with the literature, within 0.5% of previously reported data.[50-52]

Further, in order to establish a reference for the various relaxing components, we also did microwave DRS measurements on dry Nafion and poly(tetrafluoroethylene) (PTFE), shown in Fig. 1b. The dielectric response of dry Nafion (the membrane was dried extensively under vacuum at 120°C) is shown in Fig. 1b, measured at 25, 35, and 45°C. For comparison, measurements on PTFE are also displayed in this figure. The permittivity of dry Nafion (ε_s) is about 3.5, a value higher than the dielectric constant of the less-polar PTFE (ε_s = 2.0, a value which is in quantitative agreement with previous work[53]), and the dielectric loss (ε'') of dry Nafion is also higher than that of PTFE. These higher values are expected given the presence of sulfonic acid groups in Nafion. No pronounced dielectric dispersions are observed in this frequency range for either of the fluoropolymers, thus any marked relaxation that may be detected in the hydrated Nafion should correspond to mechanisms of structures involving water molecules.[c]

Results and Discussion

Strongly bound water.— Water dynamics, as well as the conductivity mechanisms, in perfluorosulfonic Nafion ionomers have been extensively investigated, with particular emphasis on dynamics much slower than those of bulk/liquid water.[37,41,54-59] Of particular interest are the studies focusing on systems with just a few water molecules, predominantly bound to the hydrophilic groups, which observe a water state that does not freeze at 0°C and vitrifies close to −100°C; this water bears spectroscopic evidence of hydrogen-bonded sulfonate/water and sulfonate/hydronium clusters, indicating proton transfer from the sulfonic groups to water.[56,57,60] It is expected that these first water molecules (λ ≤ 3) will form the first hydration shell around the sulfonate, and their dynamics should be detectable with broadband DRS. For probing the dynamics of this slow water relaxation, we focus on the low-frequency dielectric spectrum of Nafion 117 at low water content (λ = 1, Fig. 2).

Two relaxation processes contribute to permittivity losses, and both processes shift to lower frequencies by decreasing temperature (Fig. 2). The dielectric strength ($\Delta\varepsilon$) of the higher-frequency process remains constant in the entire temperature range, denoting a constant population of relaxing units [whereas the dielectric strength

[c] By design, DRS probes relaxations of dipoles from domains much larger than a single water molecule. When referring to structures involving water and loosely bound water structures, these most probably include Nafion polymer segments, specifically SO_3^- and the $-CF_2O-$ moieties, that can contribute to the dielectric relaxations recorded by both the broadband and the microwave DRS methods.

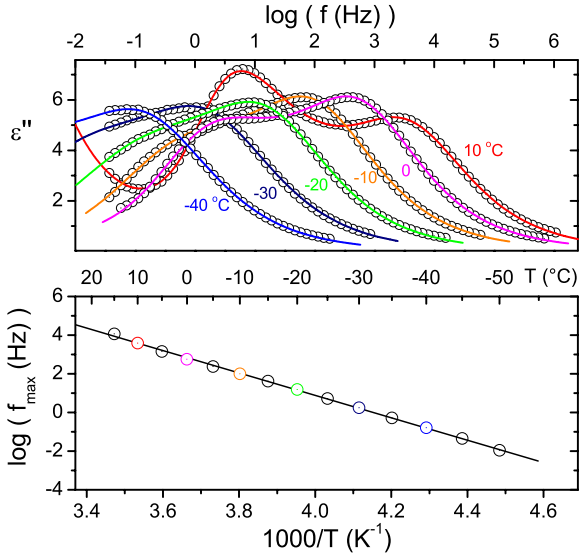

Figure 2. (Color online) (a) Dielectric loss signals for selected temperatures for Nafion 117 with λ = 1; the lines are H-N fits (Eq. A-3) to the data. The slower of the two modes is due to interfacial polarization effects, and the faster mode is attributed to the rotation of water/sulfonate groups (first hydration shell). (b) Arrhenius plot of the peak frequency (f_{max}) for the bound water relaxation over all the temperatures studied; this relaxation clearly indicates a water that does not freeze.

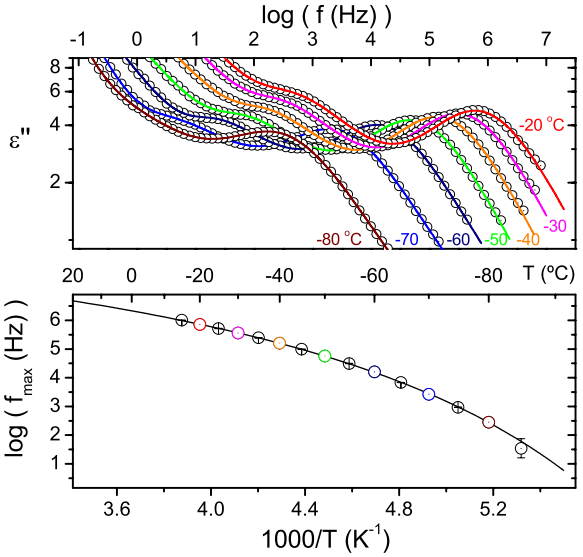

Figure 3. (Color online) (a) Dielectric loss signals for selected temperatures for Nafion with λ = 6; the lines are H-N fits to the data. The slower of the two modes is due to interfacial polarization effects, and the faster mode is attributed to the rotation of water/sulfonate structures (first and second hydration shells, SO_3^- and H_3^+O complexes). (b) Arrhenius plot of the peak frequency (f_{max}) for the bound water relaxation over all the temperatures studied; this relaxation corresponds to water structures that undergo some kind of transition (for example, this data can be described rather well by a VTFH function, indicating an apparent glass transition at 168 K).

of the lower-frequency process decreases with decreasing temperature and is described by an asymmetric Havriliak–Negami distribution of relaxation times (Appendix), corresponding to an interfacial polarization mechanism in the hydrated ionic regions[39,40]. The high-frequency process (Fig. 2) has a symmetric Cole–Cole distribution (Eq. A-1, with α = 0.4 and β = 1). Similar behavior has been reported by Pissis et al.[41,42] for Nafion-K at several hydration levels, and this mode was attributed to a dipolar β-mechanism due to the sulfonate/water cluster rotation.

The Arrhenius plot of the ε'' peak frequency (f_{max}) in the temperature range 15 to −50°C, shown in Fig. 2, reveals no change in the activation energy, denoting that the water associated with this process does not undergo a phase change, i.e., it does not form a crystalline structure, and it clearly corresponds to the nonfreezable water in Nafion.[58] The Arrhenius fit provides an activation energy of 106 ± 1 kJ/mol (cf. 1.10 ± 0.01 eV) for water in acid forms of Nafion 117 with λ = 1. This value is in good agreement with previous studies, for example, 100 kJ/mol for the ester rotation in Nafion carboxylate acid,[61] or 87 kJ/mol for Nafion-K form.[41,42] The relaxation frequency of this slowest water mode is approximately 70 kHz (cf. τ_{max} = 2.3 μs) at room temperature and becomes substantially faster at higher hydration levels, e.g., at λ = 6 (Fig. 3). These faster dynamics are mostly due to changes in the cluster morphology probed by the DRS (e.g., a second hydration shell is added to the $SO_3^-{\cdot}nH_2O$ clusters, the protons become mobile and can create macroscopic/interfacial polarizations, and DRS is probing the overall relaxation of this larger molecular aggregate) and exhibit an apparent glass transition (the water still remains nonfreezable) and/or an ice-formation transition[58] (Fig. 3). Specifically, the temperature dependence of the f_{max} from the ε'' peaks can be described rather well by a Vogel–Tammann–Fulcher–Hesse (VTFH) equation,[47,62] indicating that the water-rich clusters are governed by cooperative dynamics with an apparent glass transition at about 168 K, as calculated by the extrapolation of the fit to $\log f = -2.798$ corresponding to τ = 100 s, which is in good agreement with the transition seen in supercooled water states.[63,64] This line of research has been pursued substantially, but the exact nature/state of water in Nafion as the hydration content increases still remains unclear.[1,4,10,11,25,28-33,39-41,55-58] At this point, we limit ourselves to noting that for the lower water content in Nafion, λ = 1, the water molecules are expected to be predominately located in the first hydration layer around the sulfonate, forming a hydrated cluster with a relaxation time in the microsecond time scale at ambient temperatures. As the hydration level increases, more water molecules are added to these structures (first and second hydration shells, SO_3^-, and H_3^+O) and the dynamics of these bound waters become substantially faster, e.g., for λ = 6 the overall relaxation is in the tens of microseconds time scale at ambient temperatures. We henceforth focus on the faster states of water at ambient conditions, beyond these slow microsecond/nanosecond relaxations, and we employ dielectric microwave studies to probe these much faster dynamics.

Bulklike water and loosely bound water.— Figure 4 shows the transmission-mode permittivity spectra of various hydrated Nafion 117 at 25°C. The low-frequency divergence in ε'' (Fig. 4a) is due to the conductivity contribution in the losses following an inverse frequency (f^{-1}) dependence and resulting from the long-range motion of H_3^+O. Although it is clear from the raw data that there exists a relaxation mode at the higher frequencies, in order to obtain any quantitative information regarding this state of water in Nafion, the low-frequency conductivity contribution must be subtracted from the dielectric loss (Fig. 4b). The data analysis method is described in some detail in the Appendix.

After conductivity subtraction, the dielectric response of the hydrated Nafion samples at room temperature with λ = 3, 6, and 9 are presented in Fig. 4b, along with the fitted curves corresponding to two Debye relaxations (cf. Eq. A-7 in the Appendix). As expected, the dielectric constant of hydrated Nafion increases with increasing water content, in quantitative agreement with previous reports.[43,44] At about nine water molecules per sulfonate group (λ = 9) there is a substantial, abrupt, steplike increase in the dielectric constant, accompanied also by a similar abrupt increase in the dielectric loss ε'' (Fig. 4). This abrupt change most probably indicates the onset of percolation for the hydrophilic domains, i.e., the formation of continuous networklike structure of water paths that promote proton diffusion,[38] a supposition that is also supported by a similarly abrupt

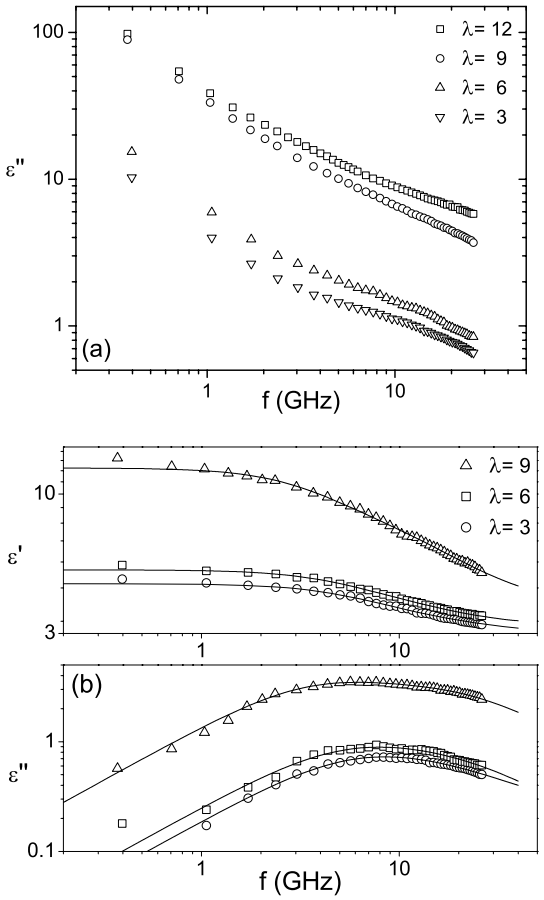

Figure 4. Permittivity vs frequency at 25°C for Nafion 117 as a function of water content (λ): (a) raw ε'' data before subtraction of the conductivity contribution and (b) ε' (raw data) and ε'' after the conductivity subtraction; the solid lines are best fits by two Debye processes.

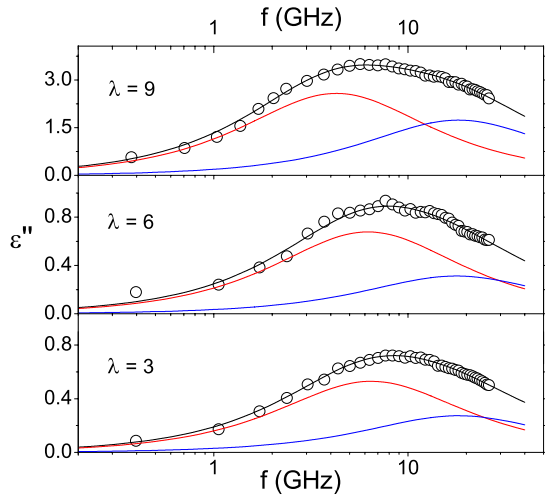

Figure 5. (Color online) Dielectric modes of water in hydrated Nafion 117 (λ = 3, 6, and 9) at 25°C. The loss $\varepsilon''(f)$ relaxation distributions and their corresponding best fits, by two Debye processes, are shown. The faster process (high frequencies) corresponds to bulklike water and the slower process (lower frequencies) to loosely bound water.

increase in the corresponding conductivity term (cf. σ_{ac} between λ = 6 and 9, Appendix, Fig. A-1) and a qualitative change in the water uptake above λ = 6 (data shown elsewhere[18,19,45,46]).

The best fit of the permittivity spectra $\varepsilon'(f)$ and $\varepsilon''(f)$ is obtained by a superposition of two Debye relaxations for $\varepsilon''(f)$, as shown in Fig. 5. The faster of the two relaxation processes coincides with the dynamics of bulklike water (Fig. 1a), with this mode's maximum at about 18 GHz, in good agreement with the microwave dielectric spectra of liquid/bulk water.[50] This relaxation process denotes that the corresponding water molecules, despite being within the Nafion membrane, are characterized by a behavior dominated by water–water hydrogen bonding and are located in regions where the local environment resembles bulk/liquid water. The lower-frequency process (Fig. 5) has a slower relaxation time than that of bulk water but is substantially faster compared to strongly bound water, i.e., compared to the process observed by the broadband dielectric spectroscopy, and was attributed to water molecules coordinated with the sulfonic groups (cf. *Strongly bound water* section). Thus, this process clearly corresponds to water molecules that are neither coordinated to sulfonic groups nor do they exhibit unconstrained/bulk liquid water dynamics. This water encompasses a broad distribution of environments within the Nafion membrane, but for the hydration levels considered in these experiments it can be argued that it would consist mostly of loosely bound water, i.e., water interacting both with free water farther away from the ionic sites and with a slower relaxing environment, such as the polymer interface or the strongly bound water molecules of the first hydration shell, resulting in an intermediate dynamic response. For example, assuming the picture provided by computer simulations for hydrated Nafion,[65,66] these loosely bound water molecules can be a second hydration shell surrounding the water coordinated to the sulfonates or, more probably, waters that reside in the hydrophilic paths connecting the hydrated ionic clusters or at the interfaces between the polymer and the bulklike liquid water (cf. hydrophobic hydration).[d]

Interestingly, with increasing water content this loosely bound water relaxation peak shifts systematically to lower frequencies for all measured temperatures (see also Fig. A-3 in the Appendix); i.e., there exists an *apparent* slow-down of the dynamics associated with the water molecules that are not coordinated to sulfonates nor are free/bulklike water molecules. This behavior most probably reflects changes in the population of the respective water state, rather than a retardation of dynamics for the same population of molecules upon further hydration. For example, regions containing water molecules characterized by this slower (20–30 ps) process upon further hydration can become extended hydrophilic regions, and their water molecules then adopt faster bulklike dynamics (8 ps); thus, they contribute to the faster process and are removed from the population of molecules of the slower process. If this happens more for the faster relaxors of the loosely bound water state (a reasonable supposition as those are located in the bigger and easier-to-hydrate regions) the distribution of dynamics of this slower process shifts to lower frequencies. Another mechanism that can account for this counterintuitive behavior is a possible increase in the population of "isolated" water, i.e., water confined within the fluorocarbon backbones,[24,67,68] which can have slower dynamics than the loosely bound water; however, for the systems of Fig. 5 we do not expect to have measurable amounts of isolated/confined water (cf. the following section).

The dielectric strengths for the two GHz water modes in Nafion

[d] Considering the microsecond relaxation times of the first hydration shell (strongly bound water molecules), attributing these loosely bound water molecules, characterized by picosecond relaxations, to the second hydration shell of the sulfonates would be striking; i.e., it seems unphysical that the two hydrations shells, despite strong hydrogen-bonding, can differ in relaxation rates by more than 5 orders of magnitude. Thus, attributing these loosely bound water molecules to be at the interfaces with polymers, either within the hydrophilic paths connecting the extended hydrophilic ion-containing domains or within these latter hydrophilic domains but closer to the polymer, seems more reasonable.

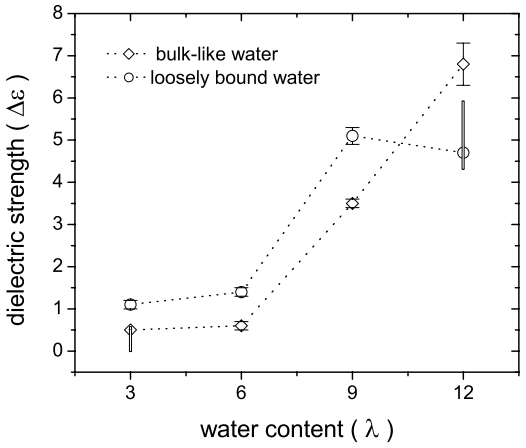

Figure 6. Dielectric strengths and the corresponding uncertainties for the two water modes (bulklike and loosely bound water) observed at gigahertz frequencies at 25°C. For the bulklike water, the bar for λ = 3 denotes the range of values that give equally good fits, including two or one relaxation modes, i.e., in the presence or absence of free water. The bar for the loosely bound water at λ = 12 is due to data scattering at low frequencies (cf. Appendix, Fig. A-2).

117 at 25°C, as derived from the data analysis,[e] are shown in Fig. 6 and summarized in Table II. The dielectric strength can be considered as a measure of the population of water molecules that contribute to a specific relaxation mode. For λ contents lower than 6, most of the membrane's water is loosely bound with small, if any, amounts of bulklike water. The loosely bound water increases with increased hydration and it levels off for λ higher than 9. Bulklike water appears in measurable quantities above λ = 6 and after that it increases almost linearly with λ, becoming dominant at the highest hydration levels.

Finally, the relaxation times of the two GHz modes observed are shown in Fig. 7 for all temperatures and water contents studied. With increasing temperature the relaxation time of both modes decreases, i.e., the relaxation modes shift to higher frequencies. The bulklike water process has almost the same relaxation time independent of hydration levels (e.g., 8.7 ps at 25°C decreasing to 5.8 ps at 45°C, for all measured values of λ = 3, 6, 9, and 12), and this value is in good agreement with the relaxation of bulk water (e.g., 8.3 ps at 25°C to 5.17 ps at 45°C when measured using the same technique, Fig. 1a) and with literature,[50] an agreement which persists at the two higher temperatures, and a posteriori further justifies the assignment of this water as bulklike liquid water within the membrane. The loosely bound water relaxation time ranges between 20 and 40 ps, depending on water content and temperature, in excellent quantitative agreement with water loosely bound to aliphatic alcohols and carboxylic acids[69] and other hydrophobic molecules.[70-72] Comparable relaxation times for water, e.g., τ_{max} = 16–30 ps, have also been reported for aqueous solutions of micelles[73] and proteins[74] and were attributed to water molecules surrounding the micellar or protein surface and interacting weakly with them, cf. loosely bound water.

From the raw data (Fig. 4 vs Fig. 1b) it is obvious that there exist at least two distinct water relaxation processes in the GHz range, which correspond to at least two distinct water environments. From the fittings of these raw data with relaxation process peaks (Fig. 5 and 7) it also becomes quite certain that one of these water environments follows the dynamics characteristic of free/bulk liquid water (cf. Fig. 1a). The second water relaxation process, assigned to loosely bound water, still in the GHz range but slower than bulk water, can correspond to many different local environments that are inherently heterogeneous in their dynamics. At first glance, it is surprising that excellent fits of this loosely bound water dynamics can be obtained by a single Debye peak, denoting a well-defined single-relaxation-time dynamic mode. Perhaps a more appropriate fitting would have been by several Debye relaxation peaks, reflecting a heterogeneity of dynamics/relaxations, a fit which is definitely mathematically possible but would have been done in an arbitrary manner given the shape of the raw data. At this point, and as we discuss next, we believe that this single relaxation time mode observed for loosely bound water is a result of our sample preparation procedure, which consisted of small hydration increments over prolonged equilibration time scales, allowing for the development of well-equilibrated morphologies within the membrane. Dielectric spectroscopy methods alone do not have enough fidelity to distinguish between all the above options or put forward any other possible explanation, and complementary morphological, dynamical, and spectroscopic studies are underway to further elucidate the exact origins and character of this water state, which is ad interim termed here as loosely bound water.

Table II. Summarized dielectric strengths (Δε) for the 25°C microwave dielectric spectra. The numbers in parentheses (for $\Delta\varepsilon_{bulklike}$ at λ = 3 and for $\Delta\varepsilon_{loosely\ bound}$ at λ = 12) are ranges of strengths for which good fits to the data can be obtained.

	$\Delta\varepsilon_{loosely\ bound}$	$\Delta\varepsilon_{bulklike}$
λ = 3	1.1 ± 0.1	(0.0–0.5)
λ = 6	1.4 ± 0.1	0.6 ± 0.1
λ = 9	5.1 ± 0.2	3.5 ± 0.1
λ = 12	(4.3–5.9)	6.8 ± 0.5

Dynamic heterogeneities of the loosely bound water.— As mentioned above, loosely bound water can exist, by definition, in many different local environments that are inherently heterogeneous in their dynamics: (*i*) one water environment with a distribution of sizes, e.g., water in hydrophilic channels of varied diameters and lengths, (*ii*) a water environment with a gradual or continuous distribution of dynamics, e.g., extended hydrophilic domains wherein the water exhibits dynamics depending on its location, accelerating from slow dynamics near the polymer/water interface to bulklike

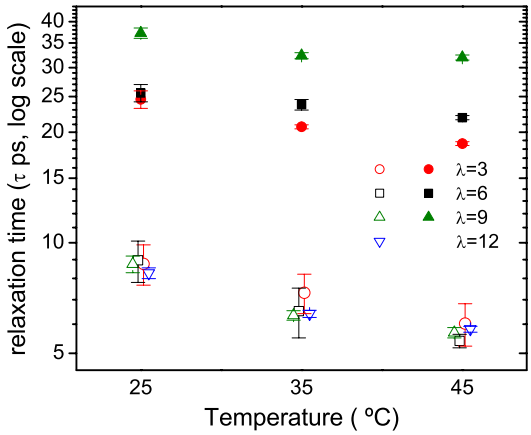

Figure 7. (Color online) The relaxation times for the bulklike (open symbols) and loosely bound (solid symbols) water states, plotted as functions of temperature and water content.

[e] For λ = 3, data analysis with a single relaxation process (assuming no bulklike water at these conditions) necessitates an asymmetric relaxation distribution, in contrast with the Debye distributions in all other cases. Analysis by two Debye processes (assuming that even at this low hydration level there exists some bulklike water) gives equally good fits for a range of strength values (Fig. 6 and Table II).

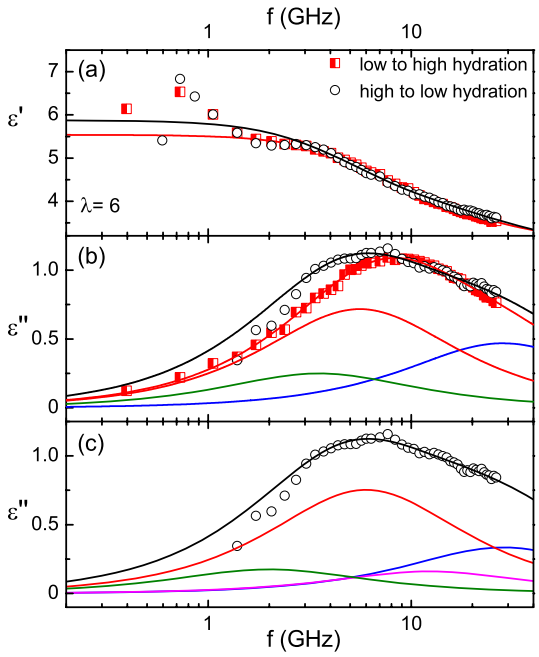

Figure 8. (Color online) Permittivity spectra at λ = 6 and 45°C for two different hydration approaches: squares correspond to a low-to-high λ change (slow water sorption), whereas circles correspond to a high-to-low λ change (drying, water desorption). Although the membrane's water content was set to λ = 6 in both cases, there exist clear differences in the dielectric response, especially in the shape of the dielectric losses, ε'', which necessitate a fit by more than two Debye processes (circles, desorption), whereas two Debye peaks provide an excellent fit for the sorption, cf. Fig. 5.

water dynamics when well inside the free water domain, or (*iii*) a variety of different environments that are characterized by similar/overlapping dynamics, e.g., hydrophilic channels, water/polymer interfaces of extended hydrophilic domains, the second hydration shell around the sulfonate/water cluster, water confined in the hydrophobic domains of the membrane, etc. The data presented so far (Fig. 5 and 7) show a remarkable single-relaxation-time process for this loosely bound water. We believe that this is a consequence of the sample preparation followed for all studies above, i.e., slight increments of λ by prolonged hydration of a lower-water-content membrane in an environment of higher relative humidity (cf. setting the λ water content by slow water sorption, allowing for the membrane morphology to reach uniformity/equilibrium). The hydration level λ only quantifies the average water content of the membrane but does not describe the distribution of water within the membrane, and consequently, the same value of λ can correspond to markedly different membrane morphologies with varied water distributions. Thus, it is possible to alter the sample-preparation approach and reach less-equilibrated membrane morphologies, which would probably more resemble the morphologies of Nafion membranes within operating fuel cells;[7] this can be done by starting with highly hydrated membranes (λ > 12) and drying them, by heating and/or under vacuum, removing water until the desired λ is reached.

In Fig. 8 we compare the permittivity spectra at 45°C for these two different hydration approaches: squares correspond to a low-to-high hydration (slow water sorption, the same approach as all previous data in this study), whereas circles correspond to the reverse approach (drying, water desorption). In both cases the membrane's water content can be set to a specified value, λ = 6 here, but there exist clear differences in the dielectric response of these two systems. Specifically, the dielectric constant ε' seems slightly higher in the drying procedure and, especially, the dielectric losses peak $\varepsilon''(\omega)$ is clearly broader, higher at low frequencies, and shows clear trends of at least a third water relaxation process (Fig. 8b and c). This last qualitative observation was checked by attempting to fit ε'' by specific relaxation processes; two Debye peaks cannot give any reasonable fitting. Relaxing the symmetry constraint for the slower peak can yield a satisfactory fit only for asymmetric peaks, which deviate in nature from all other well-defined relaxations observed here. In order to obtain reasonable fits for this broader relaxation-time distribution, a third Debye process needs to be employed (Fig. 8b); in this case, the two faster relaxation peak maxima are almost the same as before (cf. Fig. 5), whereas the third, slowest process follows a well-defined Debye relaxation distribution. As expected, equally good fits (the same quality of least-square deviations) can be obtained assuming additional Debye processes, as shown in Fig. 8c, where a fourth Debye peak with a relaxation time slightly slower than the bulklike water could develop, while keeping the raw data fitting exactly the same (the sum of the three Debye peaks in Fig. 8b is exactly the same as the sum of the four Debye peaks in Fig. 8c).

In order to better appreciate the insight provided by this last observation, one needs to consider the experimental technique. By design, dielectric spectroscopy effectively probes the rotational relaxation of a macroscopic dielectric polarization vector, which corresponds to an extended (compared to the water molecular size) sample volume. Although the relaxation of this polarization originates from individual molecular or charge motions, DRS measurements do not have the fidelity to resolve the rotation/diffusion of individual molecules or charges,[75] even without the complications due to the strong self-association of water molecules that relax via cooperative network displacements.[71,76] Thus, it is conceptually possible that the two resolved Debye processes in Fig. 5 can actually be a single water relaxation mechanism with a distribution of relaxation times, encompassing two dominating populations/structures at the observed relaxation times (cf. Fig. 7, e.g., for λ = 6 at 45°C at 6 and 22 ps). The data shown in Fig. 8 are qualitatively different in that there exists a clear broadening at the slower relaxations (τ > 20 ps), denoting either the existence of additional slower water-relaxation mechanisms or, more probably, broadening of the relaxation-time distribution toward slower relaxations. In any case, it is a clear manifestation of heterogeneities in the dynamics of water, caused by the different hydration approach, and evidently indicates the existence of water structures in Nafion with rich heterogeneous dynamics; we tentatively attribute these dynamical heterogeneities to kinetic (processing) effects on the loosely bound water structures, reflecting changes in the local environment of these water molecules.[77-79] Similar behavior can also be seen in the water uptake and the proton conductivity of Nafion when comparing between different processing approaches.[18,19,58] Given the manner by which these hydrated membrane samples (morphologies with heterogeneous dynamics) were formed, this water could not be explored systematically, because we cannot envision any systematic way to control the mass or placement of these waters with good accuracy/reproducibility.

Conclusion

DRS was carried out on Nafion 117 in the acid form at several hydration levels, and three water states were detected exhibiting distinct dynamics. In the kilohertz frequency region, we recorded a relaxation process from the rotation of hydrated sulfonate groups, depicting the dynamics of water molecules that are hydrogen-bonded to the sulfonates, cf. first and second hydration shells. This is the slowest of the water relaxations reported here; it has been observed before by others, and the present work is in quantitative agreement with these previous studies. Two additional water relaxations are observed in the gigahertz frequency region. The faster (higher frequency) process has identical dynamics with bulk/liquid water, for all Nafion hydration levels and temperatures studied, and depicts the dynamics of free, unconstrained, bulklike water within the perfluorinated anionic membranes. The second gigahertz process is slower than that of bulk/liquid water and can originate from a variety of water environments within the membrane. Here it is as-

cribed to loosely bound water, although the DRS technique employed can neither definitively trace the exact water environments being responsible for it, nor can it exclude the possibility of multiple water environments that give rise to a distribution of relaxation times. Finally, strong indications of dynamic heterogeneities of this loosely bound water were also observed here through a distinct broadening of its relaxation time distribution when a different sample preparation was followed; water was kinetically trapped within the membrane after fast water desorption. A detailed investigation of these dynamical heterogeneities could not be carried out due to our inability to systematically define hydrated regions exhibiting these dynamics.

Acknowledgments

The authors gratefully acknowledge financial support for this work by International Fuel Cells Inc. through subcontract no. 3540OB of a project by the U.S. Department of Energy contract no. DE-FC04-02AL67608. We also thank Dr. Michael Lanagan and Khalid Rajab for help and advice on microwave dielectric measurements and for critical reading of this manuscript and Mike Hickner for insightful comments on the manuscript. The broadband dielectric facilities were established through the National Science Foundation Major Research Instrumentation program (grant no. DMR-0079432). G.P. and E.M. acknowledge additional support by the Office Naval Research (grant no. 00014-05-1-0614) and the National Science Foundation (grant no. DMR-0602877).

Appendix

Dielectric data analysis

The complex permittivity data analysis can affect substantially the quantitative information, and to some extent also the qualitative trends, reported in dielectric relaxation studies. For this reason, we provide here, in some detail, the mathematics and the procedures we followed to analyze the raw data collected experimentally. In both techniques (low and high frequencies), the permittivity experimental data were fitted by two Havriliak–Negami (H-N) expressions plus a conductivity contribution[62,75,80-82]

$$\varepsilon^*(\omega) = \varepsilon_\infty + \sum_{j=1}^{2} \frac{\Delta\varepsilon_j}{[1 + (i\omega\tau_{\circ,j})^{1-\alpha_j}]^{\beta_j}} - i\frac{\sigma_\circ}{\varepsilon_\circ}\omega^{-s} \qquad [A\text{-}1]$$

resulting in the real part of the complex permittivity to be given by

$$\varepsilon'(\omega) = \varepsilon_\infty + \sum_{j=1}^{2} \frac{\Delta\varepsilon_j \cos(\beta_j\varphi_j)}{\left[1 + 2(\omega\tau_{\circ,j})^{1-\alpha_j}\sin\left(\frac{1}{2}\alpha_j\pi\right) + (\omega\tau_{\circ,j})^{2(1-\alpha_j)}\right]^{\beta_j/2}} \qquad [A\text{-}2]$$

and the imaginary part by

$$\varepsilon''(\omega) = \sum_{j=1}^{2} \frac{\Delta\varepsilon_j \sin(\beta_j\varphi_j)}{\left[1 + 2(\omega\tau_{\circ,j})^{1-\alpha_j}\sin\left(\frac{1}{2}\alpha_j\pi\right) + (\omega\tau_{\circ,j})^{2(1-\alpha_j)}\right]^{\beta_j/2}} + \frac{\sigma_\circ}{\varepsilon_\circ}\omega^{-s} \qquad [A\text{-}3]$$

where

$$\varphi_j = \arctan\left[\frac{(\omega\tau_{\circ,j})^{1-\alpha_j}\cos\left(\frac{1}{2}\alpha_j\pi\right)}{1 + (\omega\tau_{\circ,j})^{1-\alpha_j}\sin\left(\frac{1}{2}\alpha_j\pi\right)}\right] \qquad [A\text{-}4]$$

$\omega(=2\pi f)$ denotes the angular frequency, $\varepsilon_\circ$ is the vacuum permittivity, $\Delta\varepsilon$ is the dielectric relaxation strength, $\Delta\varepsilon = \varepsilon_s - \varepsilon_\infty = 2/\pi\int_0^\infty \varepsilon''(\omega)d\ln\omega$, which is a measure of the number of relaxing units; ε_s and ε_∞ are the $\varepsilon'(\omega)$ low- and high-frequency limits; $(\sigma_\circ/\varepsilon_\circ)\omega^{-s}$ is the conductivity contribution to $\varepsilon''(\omega)$, and the best fit provides $s = 1$, denoting a well-defined dc conductivity $\sigma_\circ$; the α and β peak shape parameters

$$\begin{cases} 0 \le \alpha < 1 \\ 0 < (1-\alpha)\beta \le 1 \end{cases}, \quad (1-\alpha) = \left.\frac{\partial \ln \varepsilon''}{\partial \ln f}\right|_{f\ll f_\circ}, \quad (1-\alpha)\beta = -\left.\frac{\partial \ln \varepsilon''}{\partial \ln f}\right|_{f\gg f_\circ} \qquad [A\text{-}5]$$

quantify the symmetrical and asymmetrical broadening of the loss peak, respectively, with respect to a Debye peak ($1 - \alpha = \beta = 1$); $\tau_\circ$ is a characteristic time which relates to the relaxation time $\tau_{max}(=1/2\pi f_{max})$ of each mode by

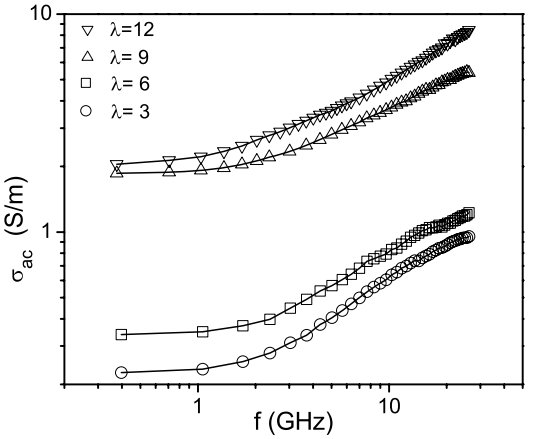

Figure A-1. Plot of the real part of conductivity (σ_{ac}), vs frequency, for Nafion 117 membrane at 25°C equilibrated at several water contents. The plateau value at low frequencies is assigned as the dc conductivity (σ_{dc}).

$$\tau_{max,j} = \tau_{\circ,j}\left[\frac{\sin(\beta_j x)}{\sin x}\right]^{1/(1-\alpha_j)} \quad \text{with} \quad x = \frac{\pi(1-a_j)}{2(1+\beta_j)} \qquad [A\text{-}6]$$

For analyzing the dipolar modes in ε'' spectra (Fig. 4a) the low-frequency conductivity contribution (linear increase of ε'') was subtracted[83] according to Eq. A-1. A best least-squares fitting procedure, based on the Levenberg–Marquardt algorithm, determines the exponent s to be equal to 1, indicating a well-defined dc conductivity (this is also clearly manifested in the values of the real part of conductivity, Fig. A-1, which are levelling off at low frequencies).

Despite the high-frequency region of the measurements, the calculated dc conductivity values derived from this data analysis (σ_{dc} = 0.23, 0.34, 1.86, and 2.05 S/m for λ = 3, 6, 9, and 12, respectively) are in good agreement with those obtained from impedance measurements in Nafion 117 at 25°C at similar water contents;[84-87] this agreement supports the usual conjecture that σ_{dc} is dominated by the mobile water dynamics. Also, it has been shown that this σ_{dc} cannot be captured by the low-frequency (broadband) dielectric measurements, because in these highly conductive Nafion systems electrode polarization and space-charge effects dominate the spectrum[88,89] (cf. Fig. 3). Finally, the possibility of ε'' increasing due to relaxation mode(s) outside and below this measurement's frequency window is rather low, because the higher frequency permittivity losses in Fig. 2 are about 2 orders of magnitude lower for the first hydration shell. Further analysis regarding conductivity effects is not discussed here because this topic, which has been extensively studied, is outside the scope of the present paper.

For the data analysis in Fig. 4b, 5, and A-3, a sum of two H-N expressions (Eq. A-2 and A-3) was used, allowing also for the fit to degenerate the two H-N theoretical curves in one, if needed. The best fit of the data provided H-N expressions with shape parameters $\alpha = 0$ and $\beta = 1$, which correspond to two symmetric Debye distributions

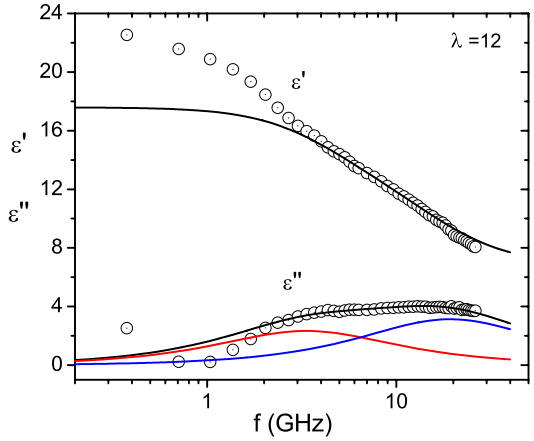

Figure A-2. (Color online) Measured permittivity $\varepsilon'(\omega)$ and absorption $\varepsilon''(\omega)$ for Nafion 117 with λ = 12 at 25°C; this membrane was equilibrated in saturated water vapor (relative humidity = 100%).

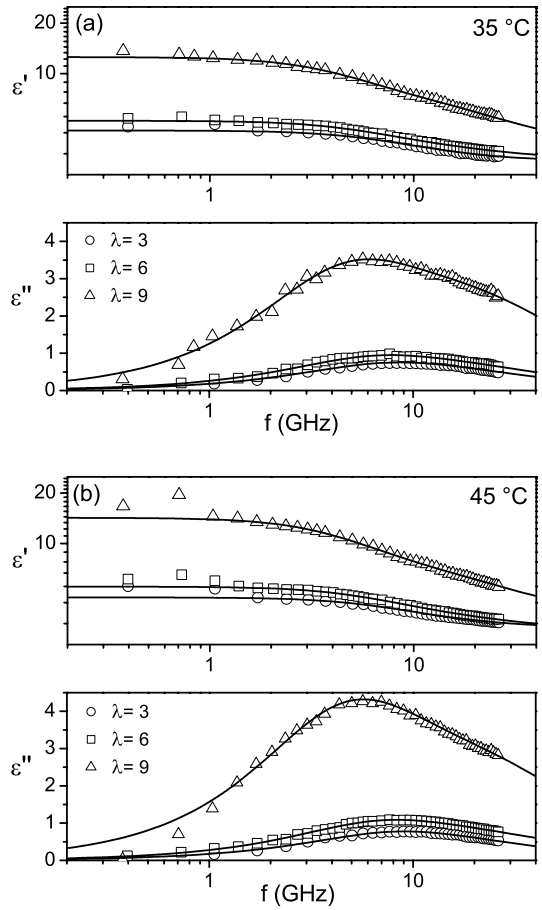

Figure A-3. Water relaxations for Nafion 117 with λ = 3, 6, and 9 at two higher temperatures: (a) 35 and (b) 45°C. In all cases, fits are by two $\varepsilon''(\omega)$ Debye peaks whose peak frequencies ($f_{max}^{-1} = 2\pi\tau_{max}$) are shown in Fig. 7.

$$\varepsilon^*(\omega) = \varepsilon_\infty + \sum_{j=1}^{2} \frac{\Delta\varepsilon_j}{1 + i\omega\tau_{\circ j}} \qquad [A\text{-}7]$$

For λ = 12 (Fig. A-2) the experimental points cannot give a satisfactory fitting throughout the frequency range due to scattering in the lower frequencies (i.e., the fits cannot capture well the lower-frequency peak), although the fit for the bulklike water mode (higher-frequency peak) is fitted with good certainty (cf. also Fig. 6)

Finally, for clarity of the figures we have presented spectra and fits at 25°C throughout the paper, although subsequently we also present and discuss data from the fits of two additonal experimental temperatures (35 and 45°C). In Fig. A-3 we provide the spectra for 35 and 45°C.

References

1. M. A. F. Robertson and H. L. Yeager, in *Ionomers, Synthesis, Structure, Properties and Applications*, Chapman and Hall, New York (1997).
2. A. D. I. Eisenberg and J. S. Kim, *Introduction to Ionomers*, John Wiley & Sons, Inc., New York (1998).
3. M. Rikukawa and K. Sanui, *Prog. Polym. Sci.*, **25**, 1463 (2000).
4. K. A. Mauritz and R. B. Moore, *Chem. Rev. (Washington, D.C.)*, **104**, 4535 (2004).
5. L. Carrette, K. A. Friedrich, and U. Stimming, *Fuel Cells*, **1**, 5 (2001).
6. M. A. Hickner and B. S. Pivovar, *Fuel Cells*, **5**, 213 (2005).
7. M. A. Hickner, N. P. Siegel, K. S. Chen, D. N. McBrayer, D. S. Hussey, D. L. Jacobson, and M. Arif, *J. Electrochem. Soc.*, **153**, A902 (2006).
8. Y. S. Kim, L. M. Dong, M. A. Hickner, T. E. Glass, V. Webb, and J. E. McGrath, *Macromolecules*, **36**, 6281 (2003).
9. M. A. Hickner, C. H. Fujimoto, and C. J. Cornelius, *Polymer*, **47**, 4238 (2006).
10. S. J. Paddison, *Annu. Rev. Mater. Res.*, **33**, 289 (2003).
11. K. D. Kreuer, S. J. Paddison, E. Spohr, and M. Schuster, *Chem. Rev. (Washington, D.C.)*, **104**, 4637 (2004).
12. J. A. Elliott and S. J. Paddison, *Phys. Chem. Chem. Phys.*, **9**, 2602 (2007).
13. R. W. Kopitzke, C. A. Linkous, H. R. Anderson, and G. L. Nelson, *J. Electrochem. Soc.*, **147**, 1677 (2000).
14. P. D. Beattie, F. P. Orfino, V. I. Basura, K. Zychowska, J. F. Ding, C. Chuy, J. Schmeisser, and S. Holdcroft, *J. Electroanal. Chem.*, **503**, 45 (2001).
15. B. Pivovar, Y. Wang, and E. L. Cussler, *J. Membr. Sci.*, **154**, 155 (1999).
16. D. Rivin, C. E. Kendrick, P. W. Gibson, and N. S. Schneider, *Polymer*, **42**, 623 (2001).
17. J. Kim, B. Kim, and B. Jung, *J. Membr. Sci.*, **207**, 129 (2002).
18. T. A. Zawodzinski, C. Derouin, S. Radzinski, R. J. Sherman, V. T. Smith, T. E. Springer, and S. Gottesfeld, *J. Electrochem. Soc.*, **140**, 1041 (1993).
19. T. A. Zawodzinski, T. E. Springer, J. Davey, R. Jestel, C. Lopez, J. Valerio, and S. Gottesfeld, *J. Electrochem. Soc.*, **140**, 1981 (1993).
20. X. Ren and S. Gottesfeld, *J. Electrochem. Soc.*, **148**, A87 (2001).
21. R. B. Moore and C. R. Martin, *Macromolecules*, **22**, 3594 (1989).
22. T. D. Gierke, G. E. Munn, and F. C. J. Wilson, *JETP Lett.*, **19**, 1687 (1981).
23. W. Y. Hsu and T. D. Gierke, *J. Membr. Sci.*, **13**, 307 (1983).
24. M. Falk, *Can. J. Chem.*, **58**, 1495 (1980).
25. K. D. Kreuer, *J. Membr. Sci.*, **185**, 29 (2001).
26. G. Gebel, *Polymer*, **41**, 5829 (2000).
27. L. Rubatat, A. L. Rollet, G. Gebel, and O. Diat, *Macromolecules*, **35**, 4050 (2002).
28. E. E. Boakye and H. L. Yeager, *J. Membr. Sci.*, **69**, 155 (1992).
29. W. A. P. Luck, *Structure of Water and Aqueous Systems*, pp. 21–72, Academic Press, New York (1984).
30. F. X. Quinn, E. Kampff, G. Smyth, and V. J. McBrierty, *Macromolecules*, **21**, 3191 (1988).
31. G. Symth, F. X. Quinn, and V. J. McBrierty, *Macromolecules*, **21**, 3198 (1988).
32. R. M. Hodge, T. J. Bastow, G. H. Edward, G. P. Simon, and A. J. Hill, *Macromolecules*, **29**, 8137 (1996).
33. H. Yoshida and Y. Miura, *J. Membr. Sci.*, **68**, 1 (1992).
34. N. Shinyashiki, M. Shimomura, T. Ushiyama, T. Miyagawa, and S. Yagihara, *J. Phys. Chem. B*, **111**, 10079 (2007).
35. N. Sivashinsky and G. B. Tanny, *J. Appl. Polym. Sci.*, **26**, 2625 (1981).
36. N. G. Boyle, V. J. McBrierty, and D. C. Douglass, *Macromolecules*, **16**, 75 (1983).
37. R. S. Chen, J. P. Jayakody, S. G. Greenbaum, Y. S. Pak, G. Xu, M. G. McLin, and J. J. Fontanella, *J. Electrochem. Soc.*, **140**, 889 (1993).
38. J. C. Perrin, S. Lyonnard, A. Guillermo, and P. Levitz, *Fuel Cells*, **1**, 5 (2006).
39. K. A. Mauritz, *Macromolecules*, **22**, 4483 (1989).
40. Z. D. Deng and K. A. Mauritz, *Macromolecules*, **25**, 2739 (1992).
41. C. Tsonos, L. Apekis, and P. Pissis, *J. Mater. Sci.*, **35**, 5957 (2000).
42. C. Tsonos, L. Apekis, and P. Pissis, *J. Mater. Sci.*, **33**, 2221 (1998).
43. S. J. Paddison, D. W. Reagor, and T. A. Zawodzinski, Jr., *J. Electroanal. Chem.*, **459**, 91 (1998).
44. S. J. Paddison, G. Bender, K. D. Kreuer, N. Nicoloso, and J. T. A. Zawodzinski, *J. New Mater. Electrochem. Syst.*, **3**, 291 (2000).
45. T. A. Zawodzinski, M. Neeman, L. D. Sillerd, and S. Gottesfeld, *J. Phys. Chem.*, **95**, 6040 (1991).
46. Z. Lu, Ph.D. Thesis, Pennsylvania State University, University Park, PA (2006).
47. N. G. McCrum, B. E. Read, and G. Williams, *Anelastic and Dielectric Effects in Polymeric Solids*, Dover Publications Inc., New York (1967).
48. M. T. Lanagan, J. H. Kim, S. J. Jang, and R. E. Newnham, *J. Am. Ceram. Soc.*, **71**, 311 (1988).
49. M. T. Lanagan, J. H. Kim, D. C. Dube, S. J. Jang, and R. E. Newnham, *Ferroelectrics*, **82**, 91 (1998).
50. W. J. Ellison, *J. Phys. Chem. Ref. Data*, **36**, 1 (2007).
51. U. Kaatze, *J. Chem. Eng. Data*, **34**, 371 (1989).
52. J. Barthel, K. Bachhuber, R. Buchner, and H. Hetzenauer, *Chem. Phys. Lett.*, **165**, 369 (1990).
53. R. G. Geyer and J. Krupka, *IEEE Trans. Instrum. Meas.*, **44**, 329 (1995).
54. S. C. Yeo and A. Eisenberg, *J. Appl. Polym. Sci.*, **21**, 875 (1977).
55. H. W. Starkweather and J. J. Chang, *Macromolecules*, **15**, 752 (1982).
56. R. Buzzoni, S. Bordiga, G. Ricchiardi, G. Spoto, and A. Zecchina, *J. Phys. Chem.*, **99**, 11937 (1995).
57. M. Ludvigsson, J. Lindgren, and J. Tegenfeldt, *Electrochim. Acta*, **45**, 2267 (2000).
58. M. Cappadonia, J. W. Erning, and U. Stimming, *J. Electroanal. Chem.*, **376**, 189 (1994).
59. J. P. Randin, *J. Electrochem. Soc.*, **129**, 1215 (1982).
60. M. Laporta, M. Pegorano, and L. Zanderighi, *Phys. Chem. Chem. Phys.*, **1**, 4619 (1999).
61. S. A. Perusich, P. Avakian, and M. Y. Keating, *Macromolecules*, **26**, 4756 (1993).
62. *Broadband Dielectric Spectroscopy*, F. Kremer and A. Schönhals, Editors, Springer, New York (2002).
63. V. Velikov, S. Borick, and C. A. Angell, *Science*, **294**, 2335 (2001).
64. P. G. Debenedetti and F. H. Stillinger, *Nature (London)*, **410**, 259 (2001).
65. R. Paul and S. J. Paddison, *Solid State Ionics*, **168**, 245 (2004).
66. R. Paul and S. J. Paddison, *J. Phys. Chem. B*, **108**, 13231 (2004).
67. M. Falk, *Structure and Properties of Ionomers* D. Reidel Publishing Co., Dordrecht, Holland (1987).
68. A. K. Lyashchenko, A. S. Lileev, T. A. Novskova, and V. S. Kharkin, *J. Mol. Liq.*, **93**, 29 (2001).
69. K. Hellenga, J. R. Grlgera, and H. J. C. Berendsen, *J. Phys. Chem.*, **84**, 2381 (1980).
70. U. Kaatze and A. Rupprecht, *J. Chem. Phys.*, **117**, 4936 (2002).
71. Y. E. Ryabov, Y. Feldman, N. Shinyashiki, and S. Yagihara, *J. Chem. Phys.*, **116**, 8610 (2002).
72. A. Lileeva, D. Loginova, A. Lyashchenko, L. Timofeeva, and N. Kleshcheva, *J. Mol. Liq.*, **131-132**, 101 (2007).
73. C. Baar, R. Buchner, and W. Kunz, *J. Phys. Chem. B*, **105**, 2906 (2001).
74. N. Nandi and B. Bagchi, *J. Phys. Chem. B*, **101**, 10954 (1997).
75. A. Boersma, J. van Turnhout, and M. Wobbenhorst, *Macromolecules*, **31**, 7453 (1998).
76. N. Agmon, *J. Phys. Chem.*, **100**, 1072 (1996).

77. J. R. Errington and P. G. Debenedetti, *Nature (London)*, **409**, 318 (2000).
78. R. M. Lynden-Bell and P. G. Debenedetti, *J. Phys. Chem. B*, **109**, 6527 (2005).
79. M. G. Mazza, N. Giovambattista, F. W. Starr, and H. E. Stanley, *Phys. Rev. Lett.*, **96**, 057803 (2006).
80. C. J. F. Boettcher and P. Bordewijk, *Theory of Electric Polarization*, Vol. 2, 2nd ed., Elsevier, Amsterdam (1978).
81. S. Havriliak and S. Negami, *Polymer*, **8**, 161 (1967).
82. F. Alvarez, A. Alegria, and J. Colmenero, *Phys. Rev. B*, **44**, 7306 (1991).
83. E. J. C. Kellar, G. Williams, V. Krongauz, and S. Yitzchaik, *J. Mater. Chem.*, **1**, 331 (1991).
84. M. C. Wintersgill and J. J. Fontanella, *Electrochim. Acta*, **43**, 1533 (1998).
85. J. J. Fontanella, M. C. Wintersgill, R. S. Chen, Y. Wu, and S. G. Greenbaum, *Electrochim. Acta*, **40**, 2321 (1995).
86. J. J. Fontanella, C. A. Edmondson, M. C. Wintersgill, Y. Wu, and S. G. Greenbaum, *Macromolecules*, **29**, 4944 (1996).
87. Y. Sone, P. Ekdunge, and D. Simonsson, *J. Electrochem. Soc.*, **143**, 1254 (1996).
88. J. J. Fontanella, M. G. McLin, and M. C. Wintersgill, *J. Polym. Sci., Part B: Polym. Phys.*, **32**, 501 (1994).
89. J. J. Fontanella, M. G. McLin, M. C. Wintersgill, J. P. Calame, and S. Greenbaum, *Solid State Ionics*, **66**, 1 (1993).